SUPPLEMENTARY DATA

SUPPLEMENTARY METHODS

Procedures – PVI+D group

Procedures were performed under general anesthesia. Antiarrhythmic medications were neither discontinued prior to ablation nor administered during the procedures. After achieving echography-guided femoral vein access, a 24-pole diagnostic catheter (Woven Orbiter, Boston Scientific Inc, United States) was placed around the tricuspid annulus with its distal part into the coronary sinus. Transseptal puncture with a conventional long sheath (SL1, Abbott Medical, United States) was performed and intravenous heparin was administered to achieve a target activated clotting time of 350 to 400 seconds. Steerable sheaths (Agilis, Abbott Medical, United States) were only used to improve catheter manipulation in selected difficult cases.

Mapping protocol and driver identification

For mapping, bipolar voltage maps were created, with the threshold for dense scar set below 0.03 mV in all navigation systems, in order to allow annotation of low-voltage signals. For driver identification on the digital recorder (LabSystem Pro, Boston Scientific Inc., United States), filters for bipolar signals were set at 30 and 250 Hz, with a notch filter.

Ablation protocol

Power settings ranged from 30 to 50 W at the LA, 30 to 40W at the RA and 20 to 30W inside the coronary sinus. Automatic ablation indexes (Lesion Size Index and Ablation Index) were used when available. For drivers at the LA, ablation lines were delivered including the drivers' location through the line in these circumstances:

a) For drivers located within or adjacent to the pulmonary veins antra, circumferential PVI was performed including the driver within the line;

b) For drivers located at the LA roof, a roof line was deployed;

c) For drivers located at the anterior LA wall, an anterior mitral line was created (from the anterior mitral annulus to the right superior or left superior pulmonary vein, or to a roof line if previously deployed, according to operators' preferences); to cover several areas with drivers, or to ablate ATs in the event of AF conversion, some patients received 2 anterior mitral lines (ie, from the mitral annulus to the right superior pulmonary vein *and* from the mitral annulus to the left superior pulmonary vein), in most cases sharing a common anterior connection to the mitral annulus (*Y-shaped* line);

d) For drivers located at the posterior wall, focal ablation was performed if the driver covered a small area; for larger drivers, a line between a right pulmonary vein and a left pulmonary vein, or a posterior box enclosing the driver (ie, roof line plus posterior line from a right pulmonary vein to a left pulmonary), was preferred; and

e) For drivers located inside the coronary sinus, focal ablation was generally performed, but coronary sinus empirical defragmentation from the ostium to the location of the driver was also valid.

Circumferential PVI was performed in all patients after ablation of LA drivers and prior to RA mapping (if performed), or during ablation of LA drivers if these were located related to the pulmonary vein antra.

After conversion to sinus rhythm, bidirectional block at the ablation lines (performed in the index or previous procedures) was checked, and ablation was performed if gaps were present. Inducibility of atrial arrhythmias was not tested at the end of the procedures.

Procedures – PVI-only group

Procedures were performed under deep sedation or general anesthesia. Antiarrhythmic drugs were managed as in the PVI+D group. In patients with circumferential radiofrequency ablation, the same ablation catheters, navigation systems and power settings as in the PVI+D were used, but without high-density mapping of the LA in most cases. After PVI, electrical cardioversion was performed to achieve sinus rhythm. Bidirectional block of all pulmonary veins was tested.

SUPPLEMENTARY RESULTS

Identification of drivers and clinical results according to the different navigation systems and mapping catheters in the PVI+D group

In the PVI+D group, 35 cases (70%) were performed using Carto3 and PentaRay NAV; 9 cases (18%) using Rhythmia and IntellaMap ORION; and 6 cases (12%) using EnSite and Advisor HD Grid. The total number of drivers (FCEs and STD+F) and the detection of regions with STD+F were similar using the 3 mapping catheters ($P = .453$ and $P = .388$, respectively). However, FCEs were more frequently found in cases performed with ORION (78%) and HD Grid (50%) than with PentaRay (31%) ($P = .039$); this means that, although all catheters seem capable of reliably detecting fractionation

and STD, ORION an HD Grid might be more prone to detecting *continuous* fractionation, possibly due to a smaller interelectrode distance and different electrode spatial configuration. However, given the limited sample size, these results must be interpreted with caution.

AF conversion rate (*P* = .344) and 1-year freedom from atrial arrhythmias (*P* = .501) were similar between the 3 navigation systems.

AF cycle length at sites with drivers and its relationship with atrial cycle length

Table 4 of the supplementary data shows the mean AF cycle length (CL) recorded at each driver (DCL), compared with the mean AF CL recorded at neighboring regions of the index atrium (ACL) without drivers, which were mapped at similar moments. Supplementary figure 3 shows representative examples and the methodology for CL measurements. Globally, there was a CL gradient between driver regions (with faster CL) and neighboring regions without drivers; the mean difference between DCL and ACL (ΔDCL–ACL) was −6.4 ± 11.9 ms, and 73% of drivers showed a shorter CL than neighboring regions. Moreover, ΔDCL-ACL was explored as a predictor of AF conversion during ablation of a particular driver site; however, it was similar for drivers in which ablation achieved AF conversion and drivers in which it was not achieved (−8.5 ± 9.5 ms vs −6.2 ± 12.2 ms, *P* = .388).

DCL was similar at sites with FCEs and sites with STD+F (162.8 ± 26.9 ms vs 158.4 ± 26.9 ms, *P* = .316); ΔDCL-ACL was also similar between the 2 driver patterns (*P* = .852), as well as for drivers in the LA, RA or coronary sinus (*P* = .432).

Mean ΔDCL-ACL was calculated for each patient (considering all drivers), and was similar for patients with and without AF conversion (−7.9 ± 6.7 ms vs −6.2 ± 5.6 ms, *P* = .358). In addition, no differences were noted between patients with or without 1-year atrial arrhythmia recurrences (−6.7 ± 5.0 ms vs −7.1 ± 6.6 ms, *P* = .840).

Finally, mean 'global' left atrial CL was explored as a possible predictor of AF conversion or arrhythmia recurrences (as shorter mean atrial CL might be related to poorer results). Mean left atrial CL was calculated as the mean of the CL of 3 different locations away from drivers, with one of these being the LAA unless drivers were adjacent to it. Mean left atrial CL was similar between patients with or without AF conversion (169 ± 17 ms vs 159 ± 21 ms, *P* = .164), and between patients with or without 1-year atrial arrhythmia recurrences (165 ± 19 ms vs 158 ± 22 ms, *P* = .315).

Methodology used for automatic fractionation maps using EnSite and Rhythmia navigation systems in the PVI+D group

For cases performed with EnSite (n = 6), the fractionation module, which automatically counts the number of deflections within the window of interest (WOI), was used. To do so, we created bipolar fractionation *turbomaps* using a low-voltage ID of 0.04 mV and a WOI comprising 90% of the AF mean CL (calculated as the mean AF CL of 3 different sites of the atrium of interest, with one of these sites being the LAA or RAA); the reason for not including 100% of the AF CL was to avoid the presence of 2 different AF EGMs within the WOI, which would be considered as the same EGM for counting deflections and could imply false fractionation detection. A threshold of 4 deflections was used for considering fractionation. Only clusters of fractionated points that created an *area* of fractionation were considered; individual scattered fractionated points were not taken into consideration. Areas < 0.5 cm away were considered as the same area of fractionation.

For cases performed with Rhythmia (n = 9), we used the LUMIPOINT module tool for automatic fractionated EGMs detection, which considers the number of deflections of *individual* EGMs, so the selection of the WOI is less relevant. Hence, we switched the LUMIPOINT module on using the same bipolar voltage maps created during mapping (ie, using the same WOI). We used the nominal threshold of 7 deflections for considering fractionation; as our definition of subjectively

detected fractionation used 4 deflections, we also explored a threshold of 4 deflections for the LUMIPOINT module, but the positive predictive value decreased without a relevant sensitivity improvement. When the LUMIPOINT module is on, areas with fractionated EGMs are highlighted; only areas with > 2 fractionated points included were counted. Areas < 0.5 cm away were also considered as the same area of fractionation.

Results according to the different ablation energy (cryoablation or radiofrequency) in the PVI-only group

As all procedures in the PVI+D group were performed with radiofrequency ablation, we performed a subanalysis considering the effect of radiofrequency vs cryoballoon ablation in the PVI-only group. A multivariate Cox proportional-hazards analysis for the primary endpoint, including study group (PVI+D vs PVI-only) and ablation energy (radiofrequency vs cryoablation) as independent variables, showed that the ablation energy was not an independent predictor of clinical results (*P* = .300 in the propensity score-matched analysis and *P* = .724 including all patients).

In the PVI-only group, similar 1-year survival free from atrial arrhythmias was observed in patients treated with radiofrequency ablation (n = 169) or cryoballoon ablation (n = 20) (*P* = .452).

Secondary analysis including all patients treated with PVI alone during the study period

In the secondary analysis that included all 189 patients treated with a PVI-only approach, the results of both primary and secondary endpoints were similar to those from the full cohort of patients (supplementary figure 4). Compared with the PVI-only group, patients in the PVI-D group had less atrial arrhythmia recurrences at 1 year of follow-up (30.6% vs 48%, log-rank *P* = .048), and at the last follow-up after one (46% vs 62%, log-rank *P* = .014) or multiple procedures (28% vs 49.7%,

log-rank *P* = .004), and experienced less progression to permanent AF (10% vs 31.2%, log-rank *P* = .003).

AF conversion to sinus rhythm (n = 3) or AT (n = 1, perimitral flutter) with ablation was observed in 4 patients (2.1%) in the PVI-only group (2.1%); in all these patients, conversion occurred during the ablation of the right superior pulmonary vein.

Results according to the operator

Procedures from the PVI+D group were performed by 4 operators, although most cases (n = 43, 86%) were performed by the same operator (operator #1). Six operators, including these 4, performed the PVI-only procedures. PVI-only procedures performed by operator #1 showed similar 1-year survival free from atrial arrhythmias to those performed by other operators (*P* = .820 in the propensity score-matched analysis and *P* = .708 including all patients). A multivariate Cox regression analysis for the primary endpoint, including study group (PVI+D vs PVI-only) and operator (operator #1 vs others) as independent variables, showed that the operator was not an independent predictor of clinical results (*P* = .532 in the propensity score-matched analysis and *P* = .518 including all patients).

SUPPLEMENTARY TABLES

Table 1 of the supplementary data: Basal characteristics including all patients.

	PVI+D (n = 50)	**PVI alone (n = 189)**	***P***
Age, y	61.2 ± 9.5	63.1 ± 10.1	.223
Female sex, %	12 (24)	46 (24)	.960
Hypertension, %	33 (66)	106 (56)	.206
Diabetes mellitus, %	13 (26)	29 (15)	.078
Obstructive sleep apnea, %	6 (12)	19 (10)	.689
Body mass index, kg/m^2	29.7 ± 4.5	29.2 ± 4.7	.476
Glomerular filtration rate, mL/min	74.5 ± 18.1	75.1 ± 17.2	.844
Left ventricular ejection fraction, %	55 [44-60]	60 [51-64]	.006
CHA_2DS_2-VASc score	2 [1-3]	2 [1-3]	.069
Indexed left atrial volume, mL/m^2	36 [29-49]	35 [30-44]	.532
Duration of the ongoing AF episode, mo	5 [3-10]	4 [3-7.5]	.511
Long-lasting persistent AF, %	11 (22)	22 (12)	.059
Significant structural heart disease , %	24 (48)	73 (39)	.230
On class I or III antiarrhythmic drugs, %	10 (20)	53 (28)	.251
Prior ablation procedures, %	17 (34)	34 (18)	.014
PVI	15 (30)	21 (11)	
CTI ablation	7 (14)	16 (8.4)	
Other	0	2 (1) *	
Prior cardiac surgery, %	4 (8)	6 (3.1)	.130

AT = atrial tachycardia. CTI = cavotricuspid isthmus. PVI+D = pulmonary vein isolation plus driver ablation. PVI = pulmonary vein isolation.

Data are shown as mean ± standard deviation, median [interquartile range] or No. (%).

* Focal AT (n = 1) and perimitral flutter (n = 1).

Table 2 of the supplementary data.

Procedural complications and mortality during follow-up.

	PVI+D (n = 50)	PVI alone (n = 50)
Complications	- Atrioesophageal fistula, n = 1 - Transient neuropathic pain at the right thigh, n = 1 - Low-risk acute pulmonary embolism during in-hospital stay, n = 1	- Phrenic nerve palsy, n = 1
Deaths and causes of death	- Atrioesophageal fistula, n = 1	- Intracranial hemorrhage, n = 1 - COVID-19, n = 1

Table 3 of the supplementary data. Detailed ablation set performed in each patient.

Patient #	Duration of ongoing AF episode, mo	Mapping catheter/ navigation system	Mapping: LA or LA + RA	Number of sites with FCEs	Number of sites with STD+F [a]	Effect of driver ablation	Ablation set	RF time, min	Atrial ablated area [b]	One-year recurrence	Progression to permanent AF
1	4	PentaRay Carto3	LA	1		AT	PVI (FCEs at RSPV)	48.6	LA: 12.3%	No	No
							CTI (conversion to common atrial flutter)	4.4			
							Focal AT at posterior wall of LA (spontaneous)	2.8			
2	2	PentaRay Carto3	LA + RA	2	3	No effect	Gap at RIPV (prior PVI)	5.8	LA: 7.8% RA: 2.3% Biatrial: 4.8%	Yes	Yes
							Focal at anteroseptal LA (FCEs)	4.9			
							Roof line (STD+F)	12.5			
							Mini-line at posterior LA to RIPV (STD+F)	4.5			
							Focal at CS ostium (FCEs)	3.1			
							Focal at lateral RA (STD+F)	1.6			
3	2	HD Grid EnSite P.	LA	1		SR	Wide gap at LSPV with FCEs (prior PVI)	18.2	LA: 3.6%	No	Yes
4	3	PentaRay Carto3	LA	0	1	No effect	PVI (prior PVI but all veins reconnected)	24.8	LA: 9.1%	Yes	No
							Roof line (STD+F)	3.1			
							ASL (induced SRSR at anterior LA)	7.7			
							CTI (prior common atrial flutter)	12.5			
5	5	PentaRay Carto3	LA + RA	0	5	No effect	PVI (STD+F at RSPV and RIPV)	26.2	LA: 16.1% RA: 4.6% Biatrial: 10.1%	No	No
							Roof line (STD+F)	8.4			
							CS defragmentation (STD+F)	6.8			
							Focal at lateral RA (STD+F)	7.4			
							CTI (transient stabilization into common atrial flutter during lateral RA ablation)	3.2			
6	2	ORION Rhythmia	LA	2		AT	PVI (FCE at RSPV)	28.6	LA: 3.3%	Yes	No
							Focal at posterolateral mitral annulus (FCEs)	4.3			
							ASL (AF conversion to SRSR at RSPV anterior antrum)	5.3			
							Focal at CS ostium (SRSR)	2.1			
7	3	PentaRay Carto3	LA	0	0	No effect	PVI (no drivers)	30.8	LA: 7.6%	No	No
8	2	PentaRay Carto3	LA + RA	2		SR	PVI	20.0	LA: 6.2% RA: 4.9% Biatrial: 5.5%	No	No
							Roof line (FCEs)	9.2			
							Cluster ablation at lateral RA (FCEs near prior atriotomy)	13.4			
9	3	PentaRay Carto3	LA + RA	2	6	No effect	Gap at LSPV (prior PVI)	7.8	LA: 11.9% RA: 8%	No	No
							ASL (FCEs antral to anterior RSPV isolation line)	9.7			

							MAL (FCEs at anterior LA near LAA base and STD+F at anterior mitral annulus)[c]	7.3	Biatrial: 9.8%		
							Roof line (STD+F)	10.9			
							Mini-line at LA floor near RIPV (STD+F)	6.3			
							Focal at CS ostium (STD+F)	5.3			
							Focal at superolateral RA (STD+F)	8.1			
							Focal at inferolateral RA (STD+F)	3.5			
10	2	HD Grid EnSite P.	LA	1		SR	PVI (FCEs at posterior carina of right PVs)	37.3	LA: 5.3%	No	No
11	4	PentaRay Carto3	LA	2	4	No effect	PVI (STD+F at RSPV and RIPV)	26.4	LA: 20.4%	Yes	No
							Posterior box: roof line (FCEs) + line between RIPV and LIPV (STD+F at posterior LA wall)	7.8			
							ASL (FCEs at anterior LA)	2.7			
							Focal at CS ostium (STD+F)	1.3			
12	10	PentaRay Carto3	LA + RA	0	5	No effect	PVI	18.6	LA: 27.9% RA: 4.7% Biatrial: 14.9%	No	No
							ASL (STD+F at anteroseptal LA)	12.6			
							MAL (STD+F at anterior LA near LAA base) [c]	2.5			
							Focal at CS ostium (STD+F)	4.8			
							Focal at septal RA (STD+F)	3.8			
							Focal at lateral RA (STD+F)	5.4			
13	2	HD Grid EnSite P.	LA + RA	0	5	No effect	PVI (STD+F at ridge)	34.2	LA: 25.9% RA: 2.8% Biatrial: 12.4%	Yes	No
							Roof line (STD+F)	4.9			
							ASL (STD+F near anterior antrum of RSPV)	11.2			
							MAL (STD+F at anterior LA near LAA base)	9.6			
							Focal at septal RA (STD+F)	3.8			
14	12	PentaRay Carto3	LA	0	3	No effect	PVI	27.8	LA: 20.3%	No	No
							Roof line (STD+F) + posterior vertical mini-line from roof line (STD+F)	7.8			
							ASL (STD+F near anterior antrum of RSPV)	9.2			
15	4	PentaRay Carto3	LA	0	3	No effect	PVI	27.8	LA: 11.2%	No	No
							Posterior box: roof line (STD+F) + line between left PVs carina and right PVs carina (STD+F at posterior LA wall)	21.9			
							MAL (STD+F at anterior LA near LAA base)	8.7			
16	3	PentaRay Carto3	LA + RA	0	8	No effect	*PVI performed in prior procedure, no gaps*		LA: 18.9% RA: 8.4% Biatrial: 13.8%	No	No
							Anterior extension of RSPV isolation line (STD+F)	12.5			
							CTI (gap from prior procedure)	5.4			
							Posterior box: roof line (STD+F) + line between RIPV and LIPV (STD+F at posterior LA wall)	22.9			
							ASL (STD+F at anterior LA)	11.6			
							Focal at posteroseptal LA near RIPV antrum (STD+F)	2.6			

							Line from high lateral RA wall to IVC (STD+F at superolateral RA and inferolateral RA)	24.6			
							Focal at CS ostium (STD+F)	4.1			
17	6	PentaRay Carto3	LA	0	3	AT	PVI (STD+F at ridge and RSPV)	55.8	LA: 15.5%	No	No
							MAL (STD+F at anterior LA)	4.8			
							ASL (AF conversion to peri-right PVs flutter)[c]	10.1			
18	2	ORION Rhythmia	LA	3		SR	*PVI performed in prior procedure, no gaps*		LA: 4.1%	No	No
							Focal at posterior roof near LSPV (FCEs)	0.5			
							ASL (FCEs at anterior mitral annulus and RSPV anterior antrum)	10.5			
							CTI (prior common atrial flutter)	4.4			
19	7	PentaRay Carto3	LA + RA	2	4	AT	PVI (FCEs at RSPV)	32.1	LA: 20.2% RA: 4.7% Biatrial: 11.8%	No	No
							Posterior line between RIPV and LIPV (FCEs)	7.9			
							ASL (STD+F anterior LA)	8.1			
							MAL (STD+F at anterior LA near LAA base)[c]	5.4			
							CS defragmentation (STD+F at ostial and mid CS)	6.1			
							Line between SVC and scar at posterior RA (AF conversion to upper loop reentry atrial flutter)	10.8			
20	1	PentaRay Carto3	LA	0	4	SR	PVI (3 sites with STD-F at RSPV, 1 at LIPV)	30.7	LA: 4.1%	No	No
							Focal at anterior RSPV antrum (spontaneous SRSR)	1.4			
21	3	PentaRay Carto3	LA + RA	2	3	No effect	Gaps at ridge and RSPV (prior PVI; FCEs at ridge)	12.8	LA: 10.2% RA: 5.8% Biatrial: 7.2%	No	No
							Roof line (FCEs)	5.5			
							"T" line between roof line and anterior mitral annulus (STD+F at anterior LA)	7.2			
							CS defragmentation (STD+F)	5.4			
							Posterior RA line between SVC and IVC (STD+F at crista terminalis)	8.6			
22	10	PentaRay Carto3	LA	5		SR	PVI (FCEs at RSPV, RIPV, LIPV and ridge)	34.2	LA: 9.9%	Yes	No
							Roof line (FCEs)	18.0			
							ASL (mechanically induced perimitral flutter)	12.6			
23	19	PentaRay Carto3	LA	0	4	AT	PVI (STD+F at RSPV)	37.1	LA: 22.1%	No	No
							Posterior box (large area with STD+F)	9.3			
							ASL (STD+F anterior LA)	10.9			
							MAL (STD+F at anterior LA near LAA base)[c]	4.9			
							CTI (AF conversion to common atrial flutter)	1.9			
24	9	PentaRay Carto3	LA + RA	0	5	No effect	PVI (STD+F at RSPV)	33.2	LA: 39.1% RA: 2.8% Biatrial:	No	No
							Posterior box (large area with STD+F)	13.5			
							MAL (STD+F at anterior LA near LAA base)	24.4			
							Focal at mitral isthmus (STD+F)	3.7			

							Focal at inferolateral RA near IVC (STD+F)	3.5	19.0%		
25	5	PentaRay Carto3	LA	0	3	AT	PVI (STD+F at RSPV)	40.6	LA: 29.1% RA: 2.4% Biatrial: 17.7%	Yes	No
							Posterior box: roof line (STD+F) + line between RIPV and LIPV (STD+F at posterior LA wall)	18.8			
							CTI (AF conversion to common atrial flutter)	4.1			
							ASL (common atrial flutter conversion to SRSR at anterior LA)	19.2			
							MAL (SRSR conversion to SRSR at LAA base)[c]	10.0			
26	11	PentaRay Carto3	LA	2	4	AT	PVI (FCEs at RSPV)	33.9	LA: 28.9%	No	No
							Posterior box: roof line (FCEs) + line between RIPV and LIPV (STD+F at posterior LA wall)	15.5			
							ASL (STD+F at anterior LA)	9.1			
							Focal at ridge (STD+F)	4.3			
							CS defragmentation (STD+F)	6.9			
							MAL (AF conversion to SRSR at LAA base)[c]	6.1			
							CTI (SRSR conversion to common atrial flutter)	3.7			
27	5	PentaRay Carto3	LA + RA	0	5	No effect	PVI (STD+F at RSPV and ridge)	43.2	LA: 14.1% RA: 1.6% Biatrial: 7.8%	Yes	Yes
							Posterior line between RIPV and LIPV (STD+F)	4.2			
							MAL (STD+F at anterior LA near LAA base)	8.3			
							CS defragmentation (STD+F)	11.7			
							Focal at CS ostium (small re-entry after electrical cardioversion of AF)	4.8			
28	4	PentaRay Carto3	LA + RA	0	4	AT	PVI	51.4	LA: 21.5% RA: 4.2% Biatrial: 14.1%	No	No
							Posterior box: roof line (STD+F) + line between RIPV and LIPV (STD+F at posterior LA wall)	10.5			
							MAL (STD+F at anterior LA near LAA)	16.7			
							CS defragmentation (STD+F)	4.1			
							CTI (conversion to common atrial flutter)	6.6			
							ASL (conversion to perimitral flutter, MAL with epicardial bridge)[c]	7.2			
29	6	PentaRay Carto3	LA	0	4	AT	PVI (STD+F at RSPV)	44.7	LA: 37.5%	Yes	No
							Posterior box (large area with STD+F)	16.4			
							ASL (STD+F at anterior LA)	18.7			
							Focal at CS ostium (STD+F)	2.0			
							Focal at posterior septum from LA + RA (AF conversion to SRSR) + mini-line to RIPV	8.7			
30	4	PentaRay Carto3	LA	1	3	AT	Gap at RIPV (prior PVI)	2.5	LA: 29.5%	No	No
							ASL (FCEs at anteroseptal LA)	12.3			
							Posterior box: roof line (STD+F) + line between RIPV and LIPV (STD+F at posterior LA wall)	24.4			
							CS defragmentation (STD+F)	5.4			

							CTI (AF conversion to common atrial flutter)	3.4			
31	6	PentaRay Carto3	LA	0	4	AT	PVI (STD+F at posterior carina of right PVs)	13.8	LA: 7.3%	No	No
							ASL (STD+F at anterior LA) + mini-extension to LAA base (incomplete "Y-shape" line) (STD+F)	11.2			
							Line at posteroseptal mitral annulus (following CS trajectory) (STD+F)	4.0			
							CTI (conversion to common atrial flutter)	7.8			
32	17	HD Grid EnSite P.	LA + RA	0	3	No effect	PVI (STD+F at RIPV)	36.3	LA: 16.1% RA: 4.4% Biatrial: 9.9%	No	No
							Posterior box (large area with STD+F)	9.6			
							CS defragmentation (STD+F)	7.7			
							CTI (common atrial flutter induced after CV)	6.0			
33	3	ORION Rhythmia	LA + RA	0	3	No effect	Gap at right middle PV (prior PVI)	2.9	LA: 12.8% RA: 3.8% Biatrial: 7.8%	No	No
							Anterior extension of prior right PV isolation line (STD+F at RIPV antrum)	7.3			
							Roof line (STD+F)	7.7			
							Posterior RA line between scars in relationship with SVC connection and IVC connection (STD+F)	6.2			
							Empirical CS defragmentation (fractionation without true STD)	2.8			
34	7	PentaRay Carto3	LA + RA	0	2	No effect	PVI	21.4	LA: 8.4% RA: 0% Biatrial: 3.3%	No	No
							ASL (STD+F at anteroseptal LA)	11.0			
							MAL (STD+F at anterior LA)[c]	4.7			
							Empirical CS defragmentation (fractionation without true STD)	7.9			
35	18	PentaRay Carto3	LA	0	2	No effect	PVI	24.9	LA: 5.7%	Yes	No
							MAL (STD+F at anterior LA)	14.9			
							Line from transeptal puncture to RIPV (STD+F)	2.6			
36	60	PentaRay Carto3	LA	0	3	No effect	PVI	21.7	LA: 7.8%	No	No
							Roof line (STD+F)	7.5			
							"T" line between roof line and anterior mitral annulus (STD+F at anterior LA)	4.7			
							Focal at posteroseptal mitral annulus (facing CS ostium) (STD+F)	3.8			
37	19	PentaRay Carto3	LA + RA	0	4	No effect	PVI	[d]	[d]	Yes	No
							Posterior box: roof line (STD+F) + line between RIPV and LIPV (STD+F at posterior LA wall)				
							ASL (STD+F at anteroseptal LA)				

							MAL (STD+F at anterior LA near LAA base) [c]				
38	3	HD Grid EnSite X	LA + RA	0	1	No effect	PVI	41.3	LA: 6.8% RA: 0% Biatrial: 3.2%	No	No
							Roof line (STD+F)	4.8			
39	38	PentaRay Carto3	LA + RA	0	1	AT	Gap at LSPV (prior PVI)	8.8	LA: 5.8% RA: 0% Biatrial: 2.7%	No	No
							ASL (STD+F at anterior LA near RSPV antrum) *AF converted into a re-entrant AT with spontaneous termination to SR*	8.6			
40	3	HD Grid EnSite X	LA + RA	1	2	AT	Anterior ablation of left PVs (wide gap from prior PVI; FCEs at left PVs carina and STD+F at superior aspect of ridge)	11.0	LA: 2.8% RA: 4.4% Biatrial: 3.8%	No	No
							Gap at RSPV (prior PVI)	2.6			
							Focal at superolateral RA (STD+F)	4.5			
							CTI (AF conversion to common atrial flutter)	3.8			
41	5	ORION Rhythmia	LA	1	2	No effect	PVI + posterior box with a single line (FCEs at posterior wall, STD+F at ridge and roof)	57.4	LA: 29.7%	No	No
							Focal at posteroseptal LA (spontaneous SRSR after CV)	3.0			
							Empirical CS defragmentation (fractionation without true STD)	5.2			
42	2	PentaRay Carto3	LA	0	0	SR	PVI (no drivers) *Spontaneous AF conversion to SR*	14.8	LA: 11.6%	No	No
43	6	ORION Rhythmia	LA + RA	2	4	No effect	PVI (FCEs at ridge and STD+F at RSPV)	39.8	LA: 9.0% RA: 0% Biatrial: 4.4%	Yes	No
							ASL (FCEs at anterior LA)	10.4			
							MAL (2 sites with STD+F at LAA base)[c]	16.6			
							CS defragmentation (STD+F)	6.9			
44	5	ORION Rhythmia	LA	0	2	No effect	PVI (STD+F at RSPV)	51.8	LA: 8.2%	No	No
							MAL (STD+F at anterior LA near LAA)	11.4			
45	15	PentaRay Carto3	LA + RA	0	4	No effect	PVI (STD+F at RIPV)	20.4	LA: 8.6% RA: 2.0% Biatrial: 5.0%	Yes	No
							Roof line (STD+F)	3.5			
							Focal at CS ostium (STD+F)	5.0			
							Focal at lateral RA (STD+F)	3.0			
46	7	ORION Rhythmia	LA + RA	4	2	No effect	Gap at RIPV (prior PVI)	5.5	LA: 16.1% RA: 2.0% Biatrial: 10.2%	Yes	Yes
							Posterior box (FCEs at posterior LA)	10.1			
							ASL (FCEs at anterior mitral annulus and anterior LA near RSPV antrum)	18.2			
							Focal at LAA anterior base (FCEs)	3.9			
							Focal at superolateral RA (STD+F)	3.4			
							Focal at inferolateral RA (STD+F)	1.0			

47	7	PentaRay Carto3	LA + RA	0	4	AT	PVI	35.2	LA: 11.7% RA: 5.0% Biatrial: 8.1%	No	No
							MAL (STD+F at anterior LA) + ASL (to achieve anterior LA block, epicardial bridge at MAL)[c]	12.6			
							Focal at superolateral RA (STD+F)	1.5			
							Focal at superoseptal RA (STD+F)	2.1			
							CS defragmentation (STD+F)	4.8			
							Focal at crista terminalis (AF conversion to SRSR)	3.7			
							CTI (conversion to common atrial flutter)	7.5			
48	5	PentaRay Carto3	LA	1	3	AT	*PVI performed in prior procedure, no gaps*		LA: 10.4%	No	No
							Anterior extension of prior right PV isolation line (FCEs at RIPV antrum, STD+F at RSPV antrum)	15.7			
							CS defragmentation (ostial STD+F) + line from LA facing CS trajectory (STD+F at posterolateral mitral annulus)	15.9			
							Focal at anterior mitral annulus (AF conversion to SRSR)	1.2			
							Focal at anteroseptal LA (SRSR conversion to another SRSR)	2.0			
							CTI (SRSR conversion to common atrial flutter)	6.5			
49	14	ORION Rhythmia	LA	1	4	No effect	PVI (FCEs at RSPV and STD+F at ridge)	36.0	LA: 8.3%	No	No
							Roof line (STD+F)	2.3			
							ASL (STD+F at anterior mitral annulus and anterior LA near RSPV antrum)	6.9			
50	84	ORION Rhythmia	LA	2	4	No effect	Gap at RIPV (prior PVI)	2.4	LA: 20.5%	Yes	Yes
							Anterior extension of prior RSPV isolation line (FCEs at antrum)	5.0			
							MAL (FCEs at LAA superior base and STD+F at LAA anterior base)	7.9			
							ASL (STD+F at superoseptal LA)	6.3			
							Posterior box (large area with STD+F)	19.7			
							CS defragmentation (STD+F)	8.2			

AF, atrial fibrillation; ASL, anteroseptal line (line between mitral annulus and right superior pulmonary vein); AT, atrial tachycardia; CS, coronary sinus; CTI, cavotricuspid isthmus; CV, cardioversion; EnSite P., EnSite Precision. FCEs, fractionated continuous or quasi-continuous electrograms; IVC, inferior vena cava; LA, left atrium; LAA, left atrial appendage; LIPV, left inferior

pulmonary vein; LSPV, left superior pulmonary vein; MAL, modified anterior line (line between mitral annulus and left superior pulmonary vein); PVs, pulmonary veins; PVI, pulmonary vein isolation; RA, right atrium; RF, radiofrequency; RIPV, right inferior pulmonary vein; RSPV, right superior pulmonary vein; SR: sinus rhythm; SRSR, scar-related small reentry; STD+F, spatiotemporal dispersion plus noncontinuous fractionation; SVC, superior vena cava.

[a] Ablation of sites with STD+F was only considered if no FCEs were found or after failed FCEs ablation. Hence, in patients with successful ablation of FCEs, this field has been codified as blank.

[b] See figure 1 of the supplementary data for the calculation method of the ablated area and examples of measurements.

[c] When an ASL and MAL were performed in the same patient, in some cases they shared the anterior connection to the mitral annulus ("Y-shape"). In the rest of cases, they were individually deployed ("V-shape").

[d] Data on regional radiofrequency times and extension of atrial ablation surface could not be obtained from this patient due to loss of back-up files from the case.

Table 4 of the supplementary data. Atrial fibrillation cycle length at location of drivers and comparison with the cycle length obtained at neighboring regions of the index atrium ('atrial cycle length') without drivers or relevant fractionation in each patient. To measure cycle length at drivers' location, adjacent electrograms without fractionation were used in order to facilitate measurement.

Patient #	Type of driver	Location	Effect of driver ablation	Driver cycle length, ms	Atrial cycle length, ms	Δ (driver cycle length - atrial cycle length)
1	FCEs	RSPV anterior antrum	**AT**	180	185	**−5**
2	FCEs	Anteroseptal LA	No effect	183	196	−13
	FCEs	CS ostium	No effect	179	196	−17
	STD+F	LA roof	No effect	171	178	−7
	STD+F	LA posterior wall	No effect	189	196	−7
	STD+F	Lateral RA	No effect	195	195	0
3	FCEs	Anterior aspect of LSPV	**SR**	178	188	**−10**
4	STD+F	LA roof	No effect	143	140	3
5	STD+F	RSPV anterior antrum	No effect	147	150	−3
	STD+F	RIPV posterior antrum	No effect	134	140	−6
	STD+F	LA roof	No effect	144	152	−8
	STD+F	CS	No effect	159	158	1
	STD+F	Lateral RA	No effect	145	157	−12
6	FCEs	RSPV anterior antrum	**AT**	163	170	**−7**
	FCEs	Posterolateral mitral annulus	No effect	149	165	−16
7	No drivers					
8	FCEs	Near LAA anterior base	**SR ***	137	155	**−18**
	FCEs	Lateral RA (prior atriotomy)	**SR ***	236	264	**−28**
9	FCEs	RSPV anterior antrum	No effect	140	136	4
	FCEs	Anterior LA near LAA base	No effect	117	124	−7
	STD+F	Anterior mitral annulus	No effect	148	148	0
	STD+F	LA roof	No effect	133	154	−21
	STD+F	LA floor near RIPV	No effect	126	129	−3
	STD+F	CS ostium	No effect	145	149	−4
	STD+F	Superolateral RA	No effect	126	162	−36
	STD+F	Inferolateral RA	No effect	150	152	−2
10	FCEs	Posterior carina or right PVs	**SR**	186	192	**−6**
11	FCEs	LA roof	No effect	129	155	−26

	FCEs	LA anterior wall	No effect	163	142	21
	STD+F	LA posterior wall	No effect	146	155	−9
	STD+F	RSPV anterior antrum	No effect	156	169	−13
	STD+F	RIPV anterior antrum	No effect	166	178	−12
	STD+F	CS ostium	No effect	161	171	−10
12	STD+F	Anteroseptal LA	No effect	141	156	−15
	STD+F	Anterior LA near LAA base	No effect	122	140	−18
	STD+F	CS ostium	No effect	155	150	5
	STD+F	Septal RA	No effect	164	168	−4
	STD+F	Lateral RA	No effect	125	140	−15
13	STD+F	LA ridge	No effect	143	152	−9
	STD+F	LA roof	No effect	157	164	−7
	STD+F	Near anterior antrum of RSPV	No effect	163	160	3
	STD+F	Anterior LA near LAA base	No effect	131	141	−10
	STD+F	Septal RA	No effect	171	176	−5
14	STD+F	LA roof	No effect	97	110	−13
	STD+F	LA posterior wall	No effect	88	121	−33
	STD+F	Near anterior antrum of RSPV	No effect	138	133	5
15	STD+F	LA roof	No effect	143	153	−10
	STD+F	LA posterior wall	No effect	154	165	−11
	STD+F	Anterior LA near LAA base	No effect	127	135	−8
16	STD+F	Near anterior antrum of RSPV	No effect	160	168	−8
	STD+F	LA roof	No effect	144	139	5
	STD+F	LA posterior wall	No effect	124	136	−12
	STD+F	LA anterior wall	No effect	142	141	1
	STD+F	Posteroseptal LA	No effect	152	143	9
	STD+F	Superolateral RA	No effect	157	168	−11
	STD+F	Inferolateral RA	No effect	163	158	5
	STD+F	CS ostium	No effect	141	169	−28
17	STD+F	LA ridge	No effect	154	162	−8
	STD+F	RSPV anterior antrum	No effect	169	179	−10
	STD+F	LA anterior wall	**AT**	163	156	**7**
18	FCEs	LA roof near LSPV	**SR**	170	181	**−11**
	FCEs	Anterior mitral annulus	No effect	165	178	−13
	FCEs	Near anterior antrum of RSPV	No effect	162	170	−8
19	FCEs	Near anterior antrum of RSPV	No effect	137	157	−20
	FCEs	LA posterior wall	**AT**	153	158	**−5**
	STD+F	Anterior LA	No effect	145	152	−7
	STD+F	Anterior LA near LAA base	No effect	163	161	2

	STD+F	CS ostium	No effect	165	163	2
	STD+F	CS	No effect	160	142	18
20	STD+F	RSPV anterior antrum	No effect	221	191	30
	STD+F	Near RSPV roof	No effect	145	183	−38
	STD+F	Near posterior RSPV antrum	No effect	150	164	−14
	STD+F	LIPV inferior antrum	**SR**	189	193	**−4**
21	FCEs	LA ridge	No effect	157	141	16
	FCEs	LA roof	No effect	128	140	−12
	STD+F	LA anterior wall	No effect	150	157	−7
	STD+F	CS	No effect	159	155	4
	STD+F	Crista terminalis	No effect	155	163	−8
22	FCEs	RSPV anterior antrum	No effect	176	192	−16
	FCEs	RIPV inferior antrum	No effect	166	187	−21
	FCEs	LIPV inferior antrum	No effect	180	178	2
	FCEs	LA ridge	No effect	174	191	−17
	FCEs	LA roof	**SR**	180	192	**−12**
23	STD+F	RSPV anterior antrum	No effect	163	144	19
	STD+F	LA posterior wall	No effect	157	175	−18
	STD+F	LA anterior wall	No effect	137	154	−17
	STD+F	Anterior LA near LAA base	**AT**	145	148	**−3**
24	STD+F	RSPV anterior antrum	No effect	170	182	−12
	STD+F	LA posterior wall	No effect	152	168	−16
	STD+F	Anterior LA near LAA base	No effect	173	158	15
	STD+F	Mitral isthmus	No effect	165	168	−3
	STD+F	Inferolateral RA	No effect	208	194	14
25	STD+F	RSPV anterior antrum	No effect	210	213	−3
	STD+F	LA roof	No effect	205	229	−24
	STD+F	LA posterior wall	**AT**	199	220	**−21**
26	FCEs	RSPV anterior antrum	No effect	144	140	4
	FCEs	LA roof	No effect	125	135	−10
	STD+F	LA posterior wall	No effect	128	120	8
	STD+F	LA anterior wall	No effect	139	136	3
	STD+F	LA ridge	**AT**	131	138	**−7**
	STD+F	CS	No effect	136	146	−10
27	STD+F	RSPV anterior antrum	No effect	198	206	−8
	STD+F	LA ridge	No effect	190	172	18
	STD+F	Anterior LA near LAA base	No effect	165	205	−40
	STD+F	LA posterior wall	No effect	169	192	−23
	STD+F	CS	No effect	177	184	−7

28	STD+F	LA roof	No effect	151	183	−32
	STD+F	LA posterior wall	No effect	149	152	−3
	STD+F	Anterior LA near LAA base	No effect	156	163	−7
	STD+F	CS	**AT**	173	177	**−4**
29	STD+F	Near anterior antrum of RSPV	No effect	153	164	−11
	STD+F	LA posterior wall	No effect	170	172	−2
	STD+F	LA anterior wall	No effect	145	168	−23
	STD+F	CS ostium	**AT**	180	201	**−21**
30	FCEs	Anteroseptal LA	No effect	238	221	17
	STD+F	LA roof	No effect	202	217	−15
	STD+F	LA posterior wall	No effect	217	233	−16
	STD+F	CS	**AT**	222	206	**16**
31	STD+F	Posterior carina of right PVs	No effect	157	168	−11
	STD+F	LA anterior wall	No effect	153	133	20
	STD+F	Anterior LA near LAA base	No effect	132	137	−5
	STD+F	Posteroseptal mitral annulus	**AT**	140	145	**−5**
32	STD+F	RIPV inferior antrum	No effect	141	150	−9
	STD+F	Posterior LA wall	No effect	136	148	−12
	STD+F	CS	No effect	165	174	−9
33	STD+F	Near anterior antrum of RIPV	No effect	126	146	−20
	STD+F	LA roof	No effect	142	150	−8
	STD+F	Posterior RA	No effect	151	153	−2
34	STD+F	Anteroseptal LA	No effect	171	179	−8
	STD+F	LA anterior wall	No effect	155	159	−4
35	STD+F	LA anterior wall	No effect	184	176	8
	STD+F	Posteroseptal LA	No effect	178	192	−14
36	STD+F	LA roof	No effect	140	154	−14
	STD+F	LA anterior wall	No effect	157	171	−14
	STD+F	Posteroseptal mitral annulus	No effect	165	179	−14
37	STD+F	LA roof	No effect	181	180	1
	STD+F	LA posterior wall	No effect	178	172	6
	STD+F	Anteroseptal LA	No effect	182	191	−9
	STD+F	Anterior LA near LAA	No effect	167	174	−7
38	STD+F	LA roof	No effect	145	157	−12
39	STD+F	Anterior LA near RSPV antrum	**AT**	132	152	**−20**
40	FCEs	Carina of left PVs	No effect	135	142	−7
	STD+F	LA ridge	No effect	141	147	−6
	STD+F	Superolateral RA	**AT**	131	140	**−9**
41	FCEs	LA posterior wall	No effect	197	165	32

	STD+F	LA ridge	No effect	184	197	−13
	STD+F	LA roof	No effect	189	173	16
42	No drivers					
43	FCEs	LA ridge	No effect	152	151	1
	FCEs	LA anteroseptal wall	No effect	165	175	−10
	STD+F	RSPV anterior antrum	No effect	152	182	−30
	STD+F	LA roof near LAA base	No effect	163	159	4
	STD+F	Anterior LA near LAA base	No effect	149	148	1
	STD+F	CS	No effect	147	157	−10
44	STD+F	RSPV anterior antrum	No effect	156	172	−16
	STD+F	Anterior LA near LAA base	No effect	140	148	−8
45	STD+F	RIPV	No effect	164	179	−15
	STD+F	LA roof	No effect	155	158	−3
	STD+F	CS ostium	No effect	188	184	4
	STD+F	Lateral RA	No effect	164	171	−7
46	FCEs	LA posterior wall	No effect	175	179	−4
	FCEs	Anterior mitral annulus	No effect	151	153	−2
	STD+F	Anterior LA near RSPV antrum	No effect	153	160	−7
	STD+F	LA near LAA anterior base	No effect	160	164	−4
	STD+F	Superolateral RA	No effect	185	172	13
	STD+F	Inferolateral RA	No effect	191	197	−6
47	STD+F	LA anterior wall	No effect	164	156	8
	STD+F	Superolateral RA	No effect	124	153	−29
	STD+F	Superoseptal RA	No effect	144	147	−3
	STD+F	CS	**AT**	146	153	**−7**
48	FCEs	RIPV inferior antrum	**AT**	173	180	**−7**
	STD+F	Near anterior antrum of RSPV	No effect	183	179	4
	STD+F	Posterolateral mitral annulus	No effect	179	174	5
	STD+F	CS ostium	No effect	184	174	10
49	FCEs	RSPV superior antrum	No effect	180	194	−14
	STD+F	LA ridge	No effect	197	193	4
	STD+F	LA roof	No effect	210	210	0
	STD+F	Anterior mitral annulus	No effect	194	200	−6
	STD+F	Anterior LA near RSPV antrum	No effect	177	201	−24
50	FCEs	Near anterior antrum of RSPV	No effect	134	140	−6
	FCEs	LAA superior base	No effect	130	136	−6
	STD+F	LA near anterior LAA base	No effect	123	136	−13
	STD+F	Superoseptal LA	No effect	142	130	12
	STD+F	LA posterior wall	No effect	139	140	−1

	STD+F	CS	No effect	159	164	−5

AT, atrial tachycardia; CS, coronary sinus; FCEs, fractionated continuous or quasi-continuous electrograms; LA, left atrium; LAA, left atrial appendage; LIPV, left inferior pulmonary vein; LSPV, left superior pulmonary vein; PVs, pulmonary veins; RA, right atrium; RAA, right atrial appendage; RIPV, right inferior pulmonary vein; RSPV, right superior pulmonary vein; STD+F, spatiotemporal dispersion plus noncontinuous fractionation.

* In this patient, ablation achieved AF conversion near the anterior base of the LAA, but AF reappeared; AF conversion was again achieved in the RA, at the superior edge of a prior atriotomy scar.

FIGURE 1 OF THE SUPPLEMENTARY DATA

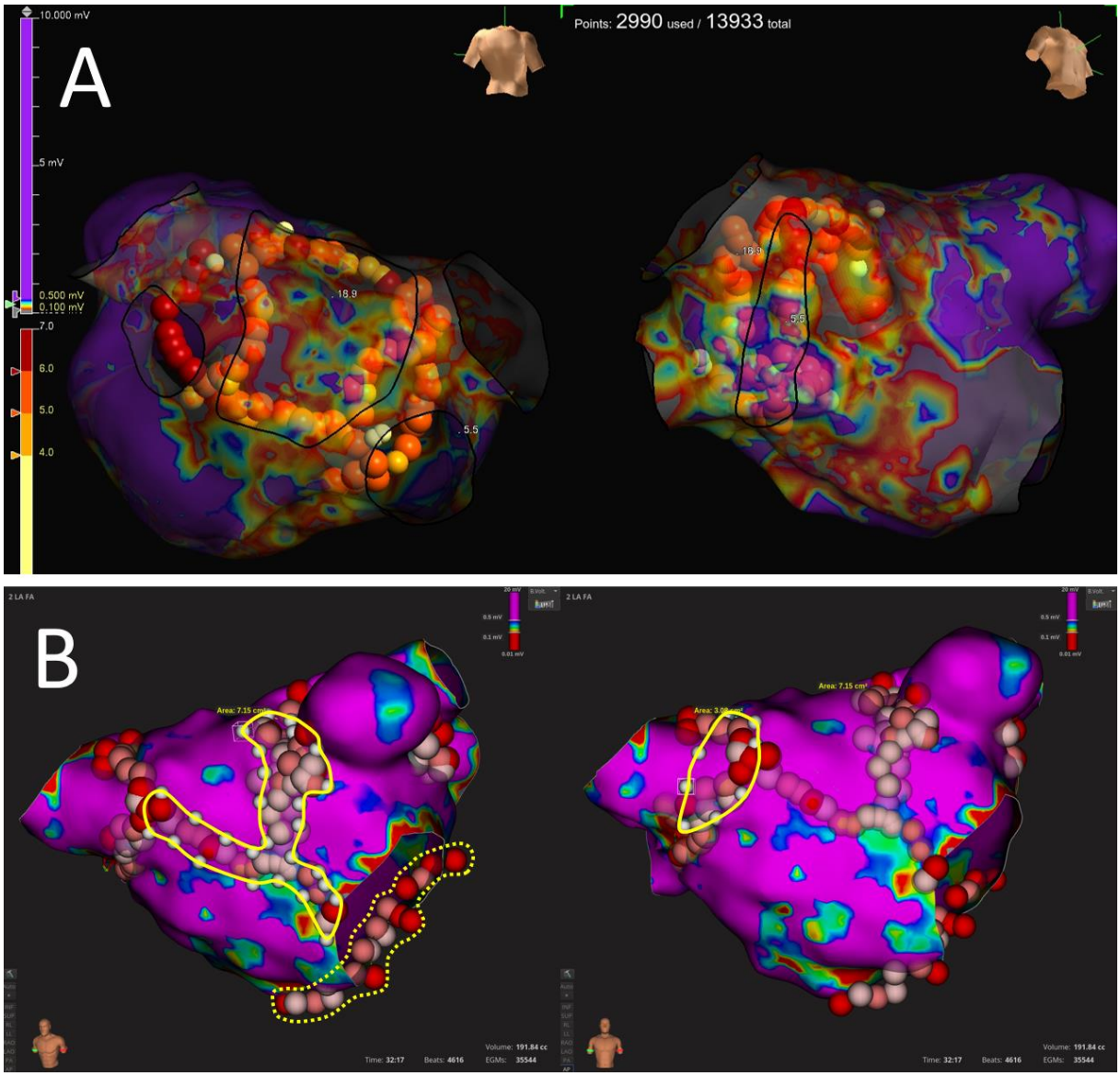

Examples of measurements of the atrial ablated area. To compute the ablated surface, lines were manually drawn on maps enclosing ablated areas using the available tools for each navigation system, and resulting areas were summed. For ablation lines, a width of ~6 mm, matching the diameter of ablation automatic marks, was used for area calculation. Electrically isolated areas due to adjacent RF lesions (eg, posterior box, antrum of pulmonary veins inside a circumferential PVI) were added into the ablated area. Pulmonary vein tissue was excluded from measurements. A) Measurements of a posterior box area and the antral aspect of the right pulmonary veins using EnSite X. B)

Measurements of a Y-shaped anterior mitral line with peri-LAA reinforcement and the antral aspect of the right superior pulmonary vein using Rhythmia; areas are highlighted using yellow solid lines for better visualization. For calculation of the ablated antral aspect of pulmonary veins, only the area *outside* an imaginary ostial PVI circumference was considered. Ablation inside the coronary sinus (as in cases with coronary sinus defragmentation) was not included in the ablated area calculation, as seen in panel B (dashed yellow line).

FIGURE 2 OF THE SUPPLEMENTARY DATA

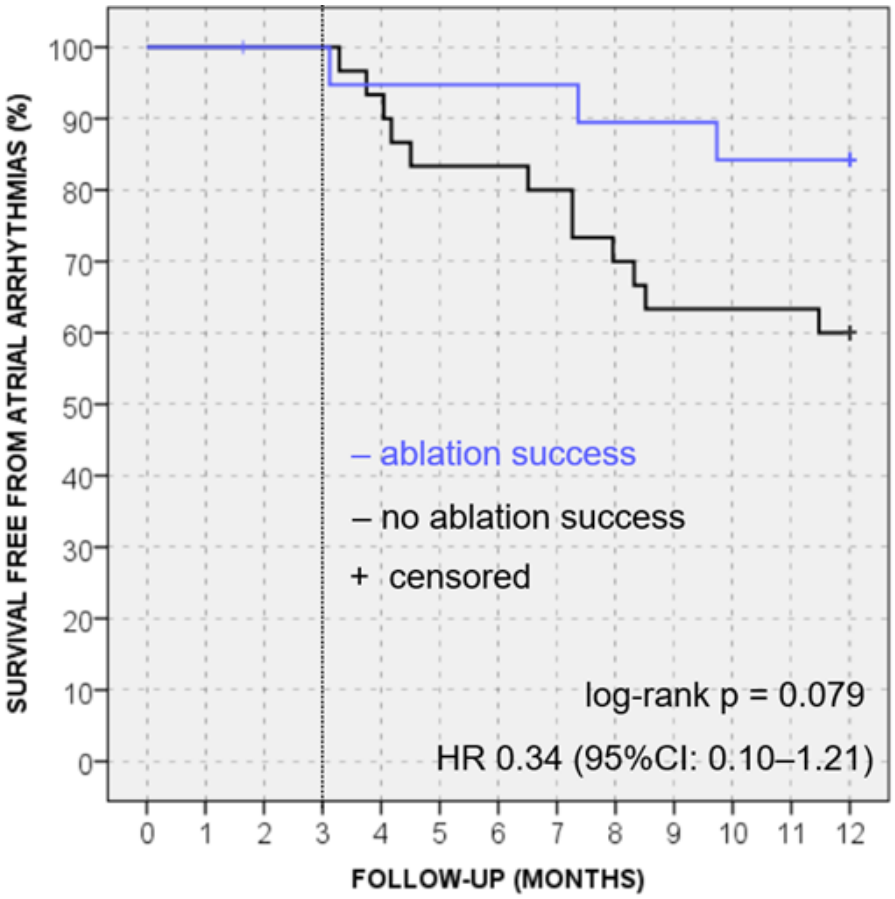

No. at risk													
Ablation success	20	20	19	19	18	18	18	18	17	17	16	16	16
No ablation success	30	30	30	30	28	25	25	24	21	19	19	19	18

Estimated 1-year survival free from atrial arrhythmias, excluding a 3-month blanking period, in patients from the pulmonary vein isolation plus driver ablation group with and without ablation success at the index procedure.

FIGURE 3 OF THE SUPPLEMENTARY DATA

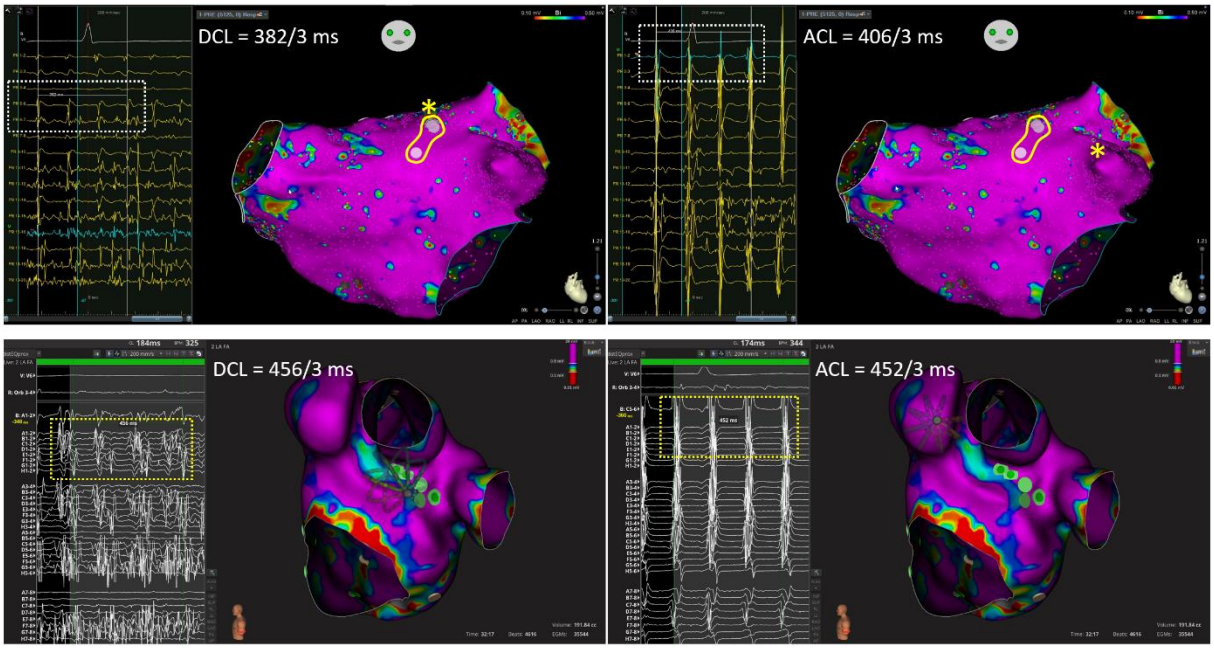

Atrial fibrillation cycle length (CL) measurements at sites with drivers (left panels) and at neighboring sites without drivers (right panels). To measure CL, the mean of 3 consecutive cycle lengths using a bipole without relevant fractionation and visually representative of the 'regional' cycle length (dashed lines) was calculated. In the upper panels (Carto3), the PentaRay position which was used for measurements is marked with an asterisk for better visualization. In the lower panels (Rhythmia), a catheter shadow shows the position of the ORION catheter. DCL, driver cycle length; ACL, atrial cycle length (cycle length measured in a near nondriver position).

FIGURE 4 OF THE SUPPLEMENTARY DATA

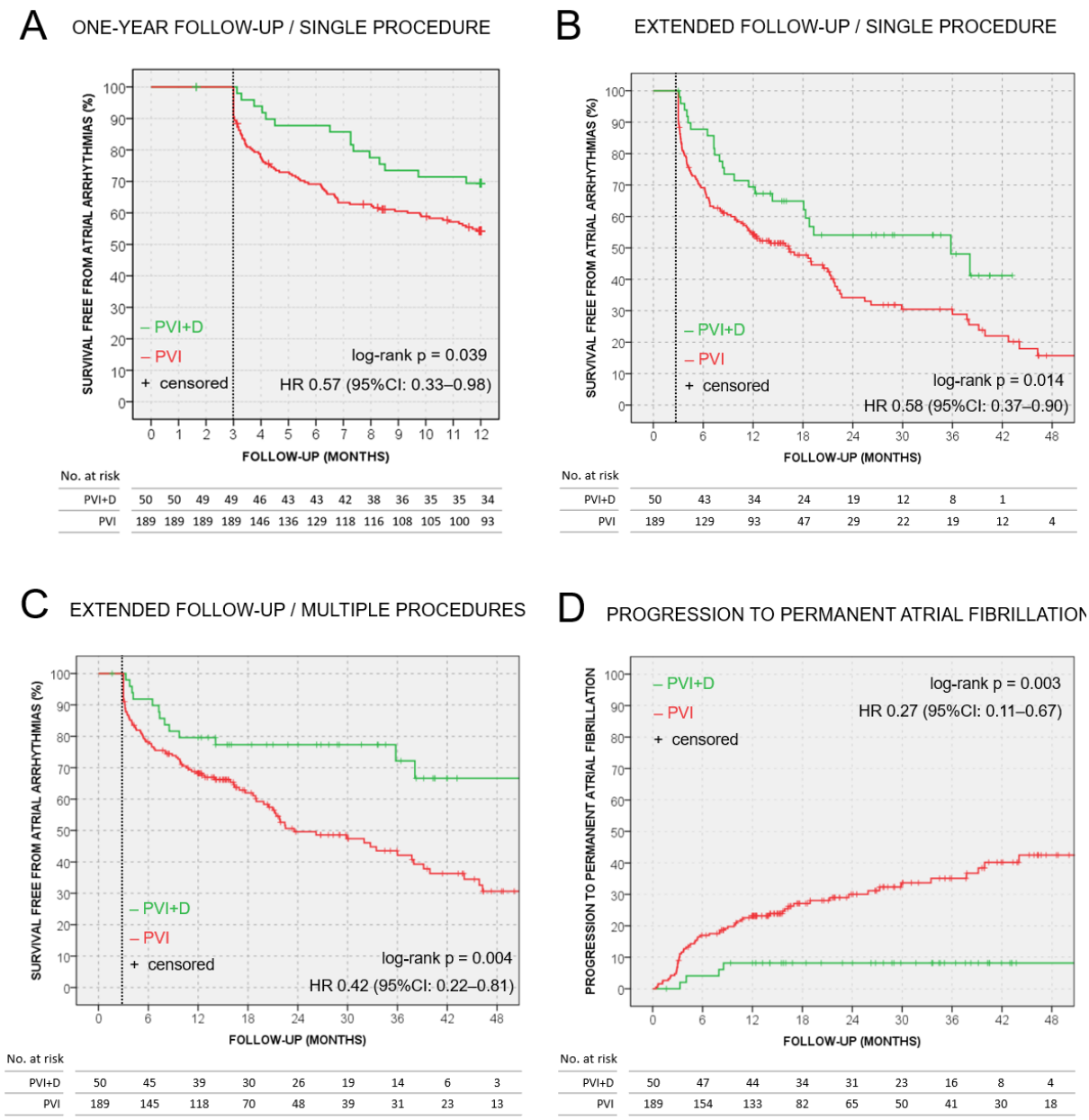

Kaplan-Meier plots of primary and secondary endpoints including all patients in the PVI-only group. A: survival free from atrial arrhythmias at 1 year of follow-up. B: survival free from atrial arrhythmia recurrences at extended follow-up. C: survival free from atrial arrhythmia recurrences at extended follow-up after multiple ablation procedures. D: progression to permanent AF. PVI+D, pulmonary vein isolation plus driver ablation group; PVI, pulmonary vein isolation-only group.